Clinics in Oncology

Review Article
Published: 29 Nov, 2016

Applications of DECT in Thoracic Oncology: Evidence So Far

*Canellas R, Digumarthy SR, Otrakji A and Kalra MK**

Department of Radiology, Massachusetts General Hospital, USA

Abstract

There is mounting evidence in favor of applying Dual Energy CT (DECT) for evaluation of suspected or known thoracic malignancies. DECT can help differentiate benign from malignant lesions of the lungs and mediastinum. Recent studies have reported role of DECT in assessing treatment response in patients with lung cancer. In this article, were view techniques and applications of DECT in thoracic oncology.

Keywords: CT; Dual energy CT; Thorax; Cancer; Treatment response

Introduction

There has been remarkable improvement in multi-detector-row CT (MDCT) technology in the last two decades. This has led to introduction of scanners with wider and faster scan coverage as well as advanced image iterative reconstruction techniques to enable reduction in CT radiation dose. There are more powerful and advanced x-ray tubes and efficient detectors in modern MDCT scanners as compared to the preceding CT technology [1,2]. These advances have enabled near simultaneous acquisition of CT images at two different energy levels or tube potential (in kilovolt age or kV) which generate the required data for Dual Energy CT (DECT).

Several applications of DECT have been reported in medical literature in the most body parts including head and neck, chest, abdomen and musculoskeletal system [3-12]. In the thorax, in addition to its vascular application in assessment of acute and chronic pulmonary embolism and thoracic aortic aneurysm and dissection, several investigators have assessed the role of DECT in evaluation of thoracic malignancies [13-16]. In this article, we review the physical principles and the applications of DECT in assessment of thoracic neoplasms.

Physical Basis and Technology of DECT

The concept of DECT is almost as old as the intervention of CT scanner originating in the 1970s with the belief that CT could enable differentiation of materials using at least two different levels of energy [17]. DECT is based on the premise that measured attenuations into data streams acquired simultaneously using low (80-100 KV) and high (140-150 KV) energy levels can provide the information to differentiate materials with high differences in their atomic mass [18]. The two-material decomposition of the DECT data sets can subtract calcium from mostly water attenuation soft tissues or iodine-based contrast media used in CT, iodine from calcium or soft tissues, and soft tissues from calcium or iodine. This separation of materials enables generation of material decomposition maps which help enhancing characteristic of the single material such as iodine maps (or in the chest, the so-called pulmonary blood volume images generated by subtracting water attenuation soft tissues [19] and virtual non-contrast images (or water images generated by subtracting iodine from the acquired data set [20]. The DECT also enables generation of virtual monochromatic images from 40-190 keV [21].

CT vendors have been adopted different technologies to generate DECT images. The earliest near simultaneous DECT capabilities were introduced on the dual source MDCT (Siemens Healthcare, Forchheim, Germany) in which the two x-ray sources operated at two different KV at the same time while scanning the same anatomic body region. This technology enables acquisition of images at each kV setting and allows use of automatic exposure control technique for radiation dose optimization [22]. However, due to differences in size of the two detector arrays, the maximal field of view is less than with single energy CT scanning (<50 cm). This can limit its application for evaluation of chest wall abnormalities or in patients with extremely large body habitus.

OPEN ACCESS

Correspondence:

Mannudeep K. Kalra, Department of Radiology, Massachusetts General Hospital, White 270, 55 Fruit Street, Boston, USA, Tel: 617 724 3192; Fax: 617 724-0046; E-mail: MKALRA@mgh.harvard.edu

Received Date: *01 Nov 2016*
Accepted Date: *22 Nov 2016*
Published Date: *29 Nov 2016*

Citation:

Canellas R, Digumarthy SR, Otrakji A, Kalra MK. Applications of DECT in Thoracic Oncology: Evidence So Far. Clin Oncol. 2016; 1: 1148.

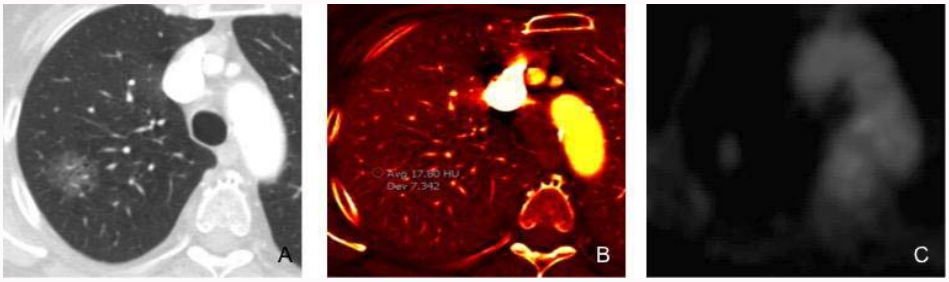

Figure 1: A 51-year-old male underwent DECT for evaluation of suspected nodular opacity on chest radiograph with subsequent PET scan (histology: adenocarcinoma *in situ*).
Figure A: The monochromatic (60 keV) image demonstrates a ground glass nodule in the right upper lobe with increased iodine uptake (1.8 mg/ml) on iodine map image (Figure B). Figure C. PET image shows low level FDG uptake (greater than the background lung uptake) in the nodule corresponding to the area of increased iodine concentration in iodine image.

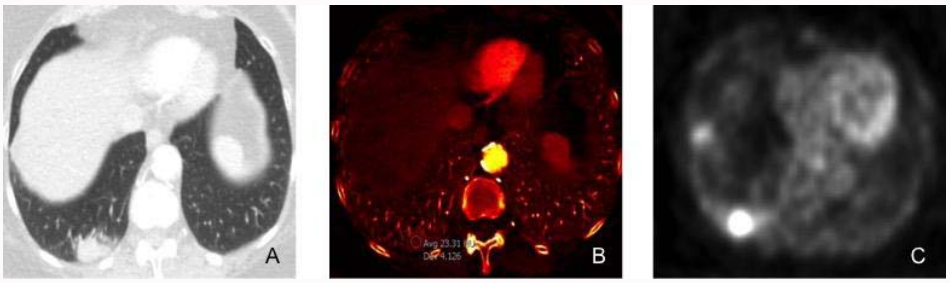

Figure 2: A 75-year-old female underwent DECT of the chest for evaluation of persistent cough, hemoptysis, and weight loss.
Figure A: DECT monochromatic 60 keV image shows right lower lobe mass.
Figure B: DECT iodine image shows high iodine distribution (2.3 mg/cc) in the right lower lobe mass.
Figure C: PET image demonstrates intense FDG uptake in the right lower lobe mass.
A CT guided fine needle biopsy of the lesion revealed adenocarcinoma of the lung.

The rapid kV switching DECT technique on single x-ray source MDCT (GE Healthcare, Waukesha, Wis.) rapidly changes the kV between 80 and 140 kV at every 0.5 millisecond. This technique enables near simultaneous acquisition of DECT in the entire 50 cm field-of-view. However, the technique does not allow use of automatic exposure control technique. Instead, users are required to select fixed tube current presets based on body regions being scanned with DECT, which may lead to higher radiation doses as compared to single energy CT particularly in the thorax [23].

The dual spin technology (Toshiba Medical Solutions, Tochigi, Japan) for DECT comprises of 2 independent sequential acquisitions at high and low KV settings. The time delay between acquisition of the 2 KV images leads to temporal miss-registration for post-contrast examinations [24].

The dual layer or sandwich detector technology (Phillips healthcare, Eindhoven, The Netherlands) based DECT involves use of layered detectors in which the 2 layers of detectors separate the low and high energy photons to generate DECT data from a single KV applied at the x-ray source [25]. Lastly, single source twin beam DECT technology (Siemens healthcare) employees a gold and tin filter to split a 120 KV x-ray beam into the low and high energy photons which are then used to generate DECT data. Compared to the dual source dual-energy CT technique, this technique enables DECT over the entire 50 cm field-of-view.

DECT Applications in Thoracic Oncology

Characterization of solitary pulmonary nodule

While thoracic CT is extremely sensitive in detection of pulmonary nodules, most of them cannot be differentiated on CT as benign or malignant. This often triggers follow-up imaging, invasive procedures and patient anxiety. Indeed, characterization of lung nodules was the first clinical application of the DECT technique. In 1994, Higashi et al. [26] reported switching of tube potential between 85 and 125 kV to generate DECT images for assessing 20 solitary pulmonary nodules and various organic solvents of different concentrations. They concluded that calcium-equivalent density images improved detection of calcification in benign nodules and virtual monochromatic images improved image quality and reliability of CT numbers. Subsequently, Bhalla et al. [27], reported improved detection of calcifications in solitary pulmonary nodules with DECT. They conducted a prospective clinical study in 27 consecutive solitary pulmonary nodules which were scanned at dual kV (80 and 140). In 11 nodules (11/27, 40%), there was an increase in the density suggesting presence of calcification (benign nature). Among these nodules, 10 (10/11, 90%) were benign and 1 (1/11, 9%) was malignant. The sensitivity of the study was 77% and the specificity 93%.

In a much larger prospective multicenter study, Swensen et al. [28] analyzed 240 nodules (86 benign and 71 malignant) using 140 kV and 80 kV x-ray beams. Since differences in mean CT numbers were not statistically significant between benign and malignant nodules, they concluded that dual-kilovolt peak analysis does not appear to be helpful in characterizing both nodules.

Following the above-mentioned studies, the new near-simultaneous DECT technologies have led to re-exploration of its application to distinguish pulmonary nodules. Chae et al. [29] evaluated 49 patients who underwent chest CT with DECT before and after contrast injection. The study demonstrated that iodine content (contrast enhancement) can successfully differentiate benign

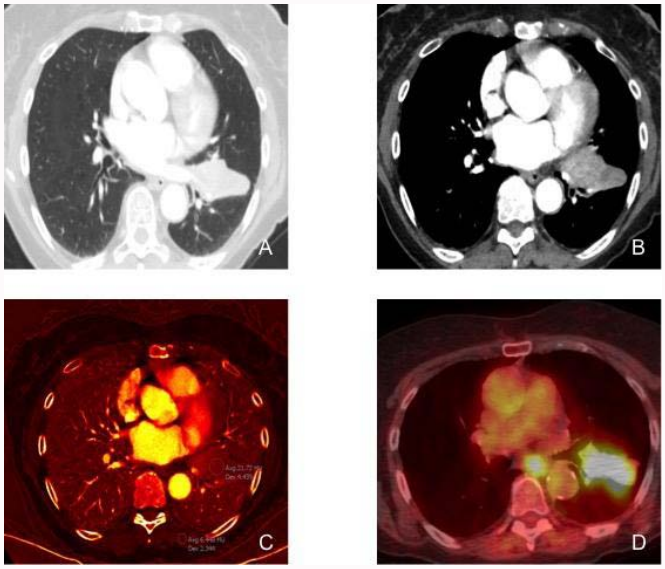

Figure 3: An 83-year-old female with stage IIIB adenocarcinoma of the left lung underwent DECT and PET/CT examination.
Figures A and B: DECT monochromatic images at 60 keV demonstrates a left lower lobe mass extending into the upper lobe across the major fissure with heterogenous contrast enhancement.
Figure C: DECT (iodine) image demonstrates high iodine distribution (2.1 mg/cc) in the lung mass. Notice the low iodine concentration in the chest wall muscle for comparison (0.6 mg/cc).
Figure D: PET/CT image demonstrates avid FDG uptake in the left lung mass, corresponding to increased iodine uptake in the DECT image.

from malignant nodules. On the basis of enhancement and CT numbers in iodine images, at 3 minutes DECT, malignant nodules demonstrated higher degree of enhancement (37 HU ± 14.6) and higher CT number (36.6 HU ± 16.0) compared to the benign nodules (17 HU ± 17.9 and 17.3 HU ± 21.8, respectively). They also found that using a cut-off value of 20 HU to characterize malignant nodules, the sensitivity, specificity and accuracy were 92%, 70% and 71.1%, respectively, for CT number and 72%, 70% and 71.1%, respectively, for degree of contrast enhancement. They also demonstrated that most calcification in nodules (17/20, 85%) and lymph nodes (44/45, 97.8%) were depicted on the Virtual Non-Contrast (VNC) images, eliminating the necessity of non-contrast CT.

In a phantom study using different concentrations of iodine and calcium, Knoss et al. [30] determined that DECT could detect iodine and calcification in artificial pulmonary nodules (n=54 nodules) ≥16 mm. In smaller nodules (< 16 mm, a clear differentiation could not be achieved. In another studying involving 24 patients, Kawai et al. [31] assessed DECT for extent of contrast enhancement in ground glass attenuation nodules. Good correlations were found between iodine concentration and calculated iodine values in the soft tissue models (r^2=0.996). Authors also reported that contrast enhancement was visible on iodine images in 22 ground glass attenuation adenocarcinomas but not in pulmonary hemorrhage and inflammatory changes (Figure 1).

Lung Cancer

Correlations between iodine measurements on DECT and histopathology of surgically resected primary lung cancers have also been found (Figure 2). In a retrospective study of 60 patients, Iwano et al. [32] assessed the correlation between iodine volume and degree of tumor differentiation (ranging from well-differentiated to undifferentiate) using a dual phase DECT protocol. The early phase was acquired using an automatic bolus tracking system and the delayed phase acquired 90 seconds after the end of the early phase. The reported mean iodine values, at the delayed phase, were 59.6 HU ± 18.6 in grade 1 tumors; 46.5 HU ± 11.3 in grade 2 tumors; 34.3 HU ± 15 in grade 3 tumors; 28.8 HU ± 6.4 in grade 4 tumors. Significant differences were observed between the four groups (p <0. 001). They also reported that iodine values at early and delayed phases were significantly correlated with tumor grade (p=0. 006 and p=0.001, respectively).

Schmid-Bindert et al. [33] assessed 37 patients with primary lung cancer who underwent DECT and 18-Fluorodeoxyglucose (18 FDG) Position Emission Tomography (PET) (Figure 3). They reported moderate correlation (r=0. 507, p=0. 025) between iodine concentration and standard uptake value (SUV_{max}) in the lung lesions. With shorter study interval of <21 days, between DECT and PET, a strong correlation was found between iodine concentration and SUV_{max} (r=0.768, p=0.017, n=17 patients) as well as in thoracic metastatic lymph nodes (r=0.654, p=0. 010).

Value of monochromatic images at 70 keV has also been assessed for differentiation of lung cancers from inflammatory masses (Figure 4). Hou et al. [34] reported differences between central and peripheral areas of pulmonary lesions with DECT at 35 seconds (arterial phase) and 90 seconds (delayed phase). HU values and normalized iodine concentrations were statistically different between the lung lesions for all assessed parameters on both arterial and delayed phases (p <0.001). Moreover, they demonstrated that a threshold of 0.34 for normalized iodine concentration can distinguish malignant and inflammatory lesions with sensitivity and specificity of 86%.

DECT has been recently used to predict post-operative pulmonary function in patients undergoing resection. Yanagita et al. [35] compared the results from single breath dual energy xenon CT (ventilation study), spirometry and perfusion SPECT. They reported that values for vital capacity and forced expiratory volume at one second by all methods regressed significantly (r^2=0.56-0.77, p <0.001 for all). Chae et al. [37] demonstrated that pre-operative

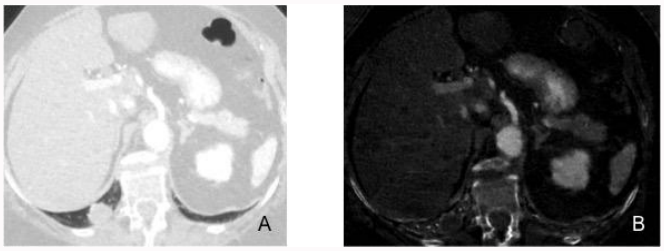

Figure 4: An 80-year-old female underwent routine chest DECT for evaluation of nodular opacity in the chest radiograph (not shown).
Figure A: DECT monochromatic image at 60 keV demonstrates a mass in the right lower lobe.
Figure B: DECT iodine image reveals a low iodine distribution in the right lower lobe mass (0.4 mg/cc), which can be seen in benign lesions. Fine needle biopsy confirmed the diagnosis of lung abscess.

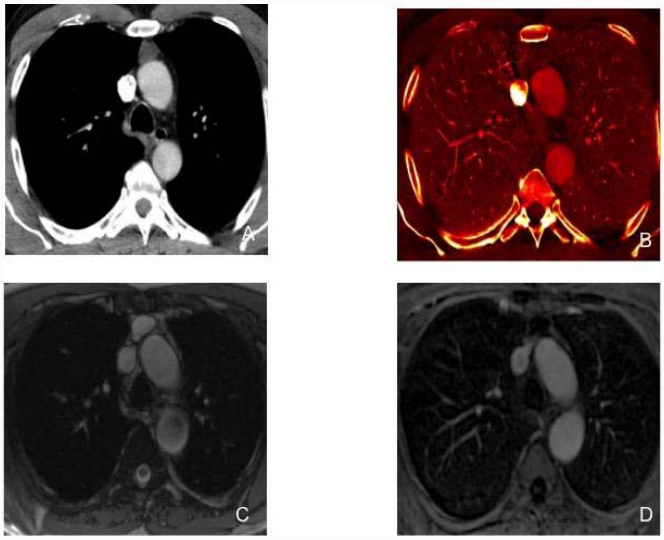

Figure 5: A 65-year-old male with myxofibrosarcoma of the anterior abdominal wall underwent routine chest DECT scan for oncologic surveillance.
Figure A: DECT (60 keV monochromatic) image demonstrates fluid attenuation lesion in the anterior mediastinum (arrow).
Figure B: DECT (iodine) image demonstrates lack of enhancement and poor iodine content (0.5 mg/cc) (hypovascular pattern) in the anterior mediastinal lesion (arrow) consistent with a thymic cyst.
Figures C and D: Follow up MRI at 1 year demonstrates stable T2 hyperintensethymic lesion with no gadolinium enhancement on T1 images in the anterior mediastinum. Stability and MR appearance confirm the cystic nature of the lesion.

DECT pulmonary blood volume maps used as "perfusion images" were more accurate than pre-operative perfusion scintigraphy for predicting post-operative pulmonary function.

The expression levels of vascular endothelial growth in non-small cell lung cancer have also been correlated with quantitative parameters from DECT. Li et al. [37] found that iodine concentration and CT values at 40keV were positively correlated with vascular endothelial growth expression score (r=0.41 and 0.39, respectively, $p < 0.05$).

Characterization of mediastinal lymph nodes

Recently, DECT has been used to differentiate benign from malignant mediastinal lymph nodes. Li et al. [37] demonstrated that DECT iodine concentration and normalized iodine concentration can be used to differentiate metastatic from non-metastatic (benign) lymph nodes in patients with non-small cell lung cancer ($p < 0.05$). With a threshold of 29.32 μg/cm^3 for iodine concentration and of 0.43 for normalized iodine concentration, authors distinguish both lymph nodes with 80% and 75% sensitivity; 70% and 75% specificity; 70% and 75% positive predictive value; 76% and 75% negative predictive value; 73% and 75% accuracy. However, no statistically significant difference was found with stratified analysis comparing different histologic tumors (adenocarcinoma and squamous cell carcinoma).

Ogawa et al. [38] assessed 83 patients who underwent DECT for evaluation of lung cancer to determine suitable scan delay for enhancement in mediastinal vessels and lymph nodes. They found that a single phase DECT acquired 60 seconds after contrast injection can replace dual-phase single energy CT protocols, which uses pre and post-contrast images. The low 80 kV images showed better contrast for identifying hilar and mediastinal lymph nodes while the weighted-average images at 120 kV were suitable to assess enhancement in pulmonary lesions. In another prospective study, Imafuji et al. [39] also proved, in suspected lung cancer patients, that 80 kV images on delayed phase (100 seconds after contrast injection) can improve detection of mediastinal and hilar lymph nodes by showing acceptable contrast and fewer beam-hardening artifacts compared to 120 kV images, acquired on early phase (30 seconds after contrast injection). These studies stress the importance of longer scan delay (>60 seconds) for acquiring DECT of the chest as compared to traditionally used 30-35 seconds scan delay for routine chest CT exams.

Characterization of mediastinal masses

The role of DECT to distinguish between malignant and

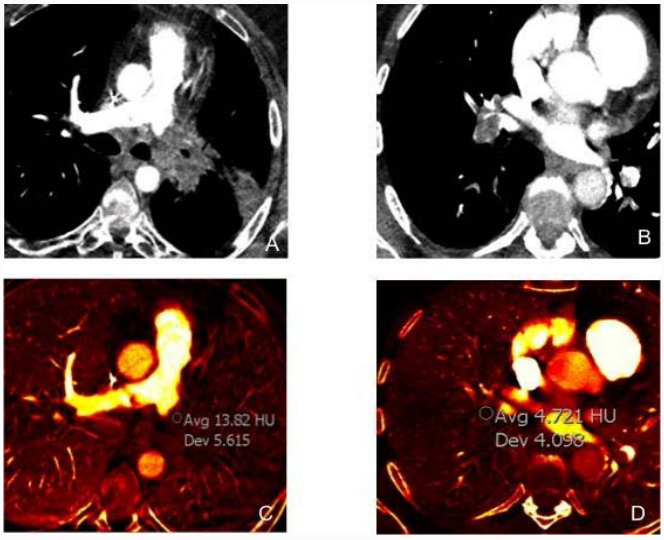

Figure 6: A 67-year-old male with left pulmonary artery sarcoma underwent DECT which demonstrated an enhancing mass involving the distal left pulmonary artery (monochromatic 60 keV image (A) with increased iodine concentration 1.3 mg/ml on iodine image (B). A complementary DECT case of a 37 year-old female with bland acute pulmonary embolus involving the right interlobar artery on monochromatic 60 keV image (C) no significant iodine concentration (0.4 mg/ml) on iodine map image (D).

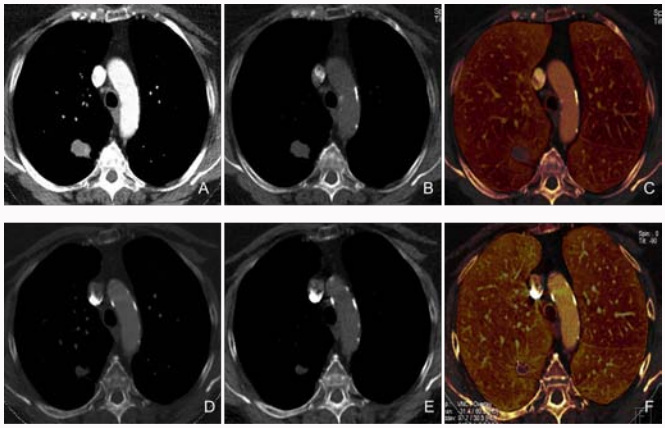

Figure 7: A 67-year-old female with a history of lung adenocarcinoma underwent DECT before and after chemotherapy over a three month interval.
Pre-treatment DECT images monochromatic 60 keV (A), virtual non-enhanced (B), iodine (C) demonstrate enhancing nodule in the right lower lobe with iodine concentration of 2.1 mg/ml. The post-treatment DECT images monochromatic 60 keV (D), virtual non-enhanced (E), iodine (F) demonstrate treatment response with decrease in the size of the nodule and reduced iodine concentration (1.1 mg/ml).

benign mediastinal tumors has also been assessed (Figure 5). In a prospective study Lee et al. [40] performed a prospective study of 50 patients and reported that iodine concentration and iodine related HU (iodine-enhanced HU value – non-enhanced HU value) were significantly different and higher in malignant mediastinal lesions compared to benign lesions ($p < 0.001$). Significant differences were noted on both early (15 seconds after the peak of enhancement in the main pulmonary artery) and delayed phases (40 seconds after the early phase). However, traditional CT numbers did not show any statistically significant difference. The best cut-off iodine concentration value to differentiate benign from malignant lesions was 1.40 mg/mL for the early phase DECT and 1.58 mg/mL for the delayed phase DECT. The respective sensitivity, specificity and area under the curve for diagnosing malignant mediastinal tumors with DECT were 93.3%, 90% and 0.887 for the arterial phase and 100%, 80% and 0.887 for the delayed phase.

In another small study (n=25 patients), Chang et al. [41] reported successful differentiation of pulmonary artery sarcoma from pulmonary thromboembolism with DECT (Figure 6). They reported that mean iodine-related HU (27.9 HU ± 9.1 *vs.* 10.6 ± 7.2, p=0.004) and mean iodine concentration (1.49 mg/mL ± 0.57 *vs.* 0.61 mg/mL ± 0.39, p=0.001) were significantly higher in the cancer group compared to thromboembolic group. The reported areas under the curve were 0.934 (95% CI, 0.759-0.991, $p < 0.001$) for iodine-related HU value and 0.912 (95% CI, 0.729-0.986, p=0.001) for iodine concentration value. No statistically significant differences were found using HU to differentiate the lesions.

Assessing cancer response to treatment

Assessment of early treatment response is extremely important in adjusting, continuing and discontinuing treatment regimens in order to minimize treatment risk and maximize anticipated benefits (Figure 7). Value of iodine uptake on DECT images in assessment of treatment response has been evaluated in patients with lung cancer. In a retrospective study using a dual-phase DECT protocol, Baxa et al. [42] demonstrated that arterial enhancement fraction assessed in pre- and post-treatment lymph nodes (n=110 patients) can be used

to predict the effectiveness of chemotherapy in patients with non small cell lung cancers. There was a significant decrease in arterial enhancement fraction in responding lymph nodes (26%, p=0.022) and a significant increase in non-responding lymph nodes (43%, p=0.031). In this study, the early phase DECT images were acquired 5 seconds after the attenuation in distal aorta increased to 100 HU while the delayed phase DECT images were acquired 15 seconds after the end of the early phase.

Statistically significant difference in percentage change in arterial enhancement fraction between responders and non-responders (p=0.019-0.043) has also been reported with DECT in patients with non small cell lung cancers before and after treatment with anti-EGFR drugs [43]. The study included 31 patients who underwent dual-phase DECT with early phase scan at 5 seconds after the attenuation in distal aorta increased to 100 HU and the late phase at 20 seconds after the end of the early phase.

Kim et al. [44] have reported that iodine maps and virtual non-contrast images from DECT can be used to assess tumor response after anti-angiogenic (bevacizumab) in non small cell lung cancer. Tumor response was evaluated using Choi (reflecting net tumor enhancement assessed with iodine maps) and RECIST (reflecting size changes only) criteria. A good agreement (k=0.72) between both criteria was found. DECT images improved the response evaluation by preventing mischaracterization of progressive disease in cases with hemorrhage leading to tumor growth.

Level of Evidence for Application of DECT in Thoracic Neoplasms

Review of published literature on DECT is encouraging for its applications for characterization of solitary pulmonary nodules and mediastinal lesions, as well as for assessment of treatment response. Nevertheless, these preliminary studies need to be interpreted with some caveats. Firstly, the small number of patients in single center settings and the retrospective nature of most DECT studies can lead to unintentional selection bias. Prospective studies in larger populations in multicenter settings are still lacking. Reliability of some studies, especially those involving iodine concentration measurements, has not been tested in uncontrolled clinical settings. It is also not clear how use of different DECT technologies from different vendors can affect both quantitative and qualitative results. Additional investigations are needed to assess if iodine measurements and HU values from DECT images remain stable with changes in contrast injection protocols and patients related factors such as fluid overload, cardiac output as well as phase of breath hold during scanning. These issues have plagued the reproducibility and reliability of single energy related CT measurements.

Furthermore, publications and applications of dual-phase DECT of the chest warrant careful assessment of applied radiation doses since some DECT technologies are associated with increased radiation dose levels compared to single energy CT studies. Increased radiation dose from dual phase DECT protocols is a legitimate concern in young patients without established history of cancer. In such subjects, stringent verification of DECT applications is needed along with focused development of low radiation dose DECT protocols.

Future Directions

Initial studies have uniformly demonstrated potential applications of DECT in thoracic oncology. It is hoped that larger multicenter trails will help further the evidence in favor of DECT as the technology becomes more widely available.

Photon-counting detector CT technology has been recently used for phantom and in human cadavers and human volunteers [45-47]. This technique counts individual photon interactions using high-speed semiconductors (without the need of scintillator crystals) and allows simultaneous measurements of the energy and number of photons. Pourmorteza et al. [48] prospectively enrolled 15 patients and scanned their abdomen using photon-counting detector. Quantitative and qualitative image parameters were assessed and compared to CT scanners that use energy-integrating detectors (used in all commercially available CT). The results showed similar qualitative scores for image quality, noise and artifacts ($p > 0.05$). Iodine and virtual non-contrast images showed better contrast-to-noise ratio in the former group by an average of 32% ($p < 0.001$). Initial results with photon count detector CT technology show promise but its advantages over DECT from current multidetector-row CT remain unproven. In addition, currently photon-counting detector is a rather niche technology which is extremely expensive and computationally challenging.

Another field being explored with DECT is its application in radiation treatment planning. The improvement in image quality and tissue characterization provided by DECT technology, improve dose calculation in brachytherapy, to accurate estimate the stop power ratio in proton therapy and to allow better estimation of electron density in photon therapy [49,50].

Conclusion

DECT represents a promising technique for evaluation of a variety of thoracic lesions. Several publications have documented its usefulness in differentiation of benign and malignant thoracic lesions and in assessment of treatment response in patients with lung cancers.

References

1. Petersilka M, Bruder H, Krauss B, Stierstorfer K, Flohr TG. Technical principles of dual source CT. Eur J Radiol. 2008; 68: 362-368.
2. Johnson TR. Dual-energy CT: general principles. AJR Am J Roentgenol. 2012; 199: S3-S8.
3. Flohr TG, McCollough CH, Bruder H, Petersilka M, Gruber K, Süss C, et al. First performance evaluation of a dual-source CT (DSCT) system. Eur Radiol. 2006; 16: 256-268.
4. Otrakji A, Digumarthy SR, Lo Gullo R, Flores EJ, Shepard JA, Kalra MK, et al. Dual-Energy CT: Spectrum of Thoracic Abnormalities. Radiographics. 2016; 36: 38-52.
5. Godoy MC, Naidich DP, Marchiori E, Assadourian B, Leidecker C, Schmidt B, et al. Basic principles and postprocessing techniques of dual-energy CT: illustrated by selected congenital abnormalities of the thorax. J Thorac Imaging. 2009; 24: 152-159.
6. Marin D, Boll DT, Mileto A, Nelson RC. State of the art: dual-energy CT of the abdomen. Radiology. 2014; 271: 327-342.
7. Spek A, Strittmatter F, Graser A, Kufer P, Stief C, Staehler M. Dual energy can accurately differentiate uric acid-containing urinary calculi from calcium stones. World J Urol. 2016.
8. Ginat DT, Mayich M, Daftari-Besheli L, Gupta R. Clinical applications of dual-energy CT in head and neck imaging. Eur Arch Otorhinolaryngol. 2016; 273: 547-553.
9. Hixson HR, Leiva-Salinas C, Sumer S, Patrie J, Xin W, Wintermark M. Utilizing dual energy CT to improve CT diagnosis of posterior fossa ischemia. J Neuroradiol. 2016.

10. Yamauchi H, Buehler M, Goodsitt MM, Keshavarzi N, Srinivasan A. Dual-Energy CT-Based Differentiation of Benign Posttreatment Changes From Primary or Recurrent Malignancy of the Head and Neck: Comparison of Spectral Hounsfield Units at 40 and 70 keV and Iodine Concentration. AJR Am J Roentgenol. 2016; 206: 580-587.

11. Omoumi P, Becce F, Racine D, Ott JG, Andreisek G, Verdun FR. Dual-Energy CT: Basic Principles, Technical Approaches, and Applications in Musculoskeletal Imaging (Part 1). Semin Musculoskelet Radiol. 2015; 19: 431-437.

12. Sun X, Shao X, Chen H. The value of energy spectral CT in the differential diagnosis between benign and malignant soft tissue masses of the musculoskeletal system. Eur J Radiol. 2015; 84:1105-11058.

13. Paul J, Vogl TJ, Mbalisike EC. Oncological applications of dual-energy computed tomography imaging. J Comput Assist Tomogr. 2014; 38: 834-842.

14. Agrawal MD, Pinho DF, Kulkarni NM, Hahn PF, Guimaraes AR, Sahani DV. Oncologic applications of dual-energy CT in the abdomen. Radiographics. 2014; 34: 589-612.

15. Lam S, Gupta R, Kelly H, Curtin HD, Forghani R. Multiparametric Evaluation of Head and Neck Squamous Cell Carcinoma Using a Single-Source Dual-Energy CT with Fast kVp Switching: State of the Art. Cancers (Basel). 2015; 7: 2201-2216.

16. Remy-Jardin M, Faivre JB, Pontana F, Hachulla AL, Tacelli N, Santangelo T, et al. Thoracic applications of dual energy. Radiol Clin North Am. 2010; 48: 193-205.

17. Marshall WH, Jr, Easter W, Zatz LM. Analysis of the dense lesion at computed tomography with dual kVp scans. Radiology. 1977; 124: 87-89.

18. Liu X, Yu L, Primak AN, McCollough CH. Quantitative imaging of element composition and mass fraction using dual-energy CT: three-material decomposition. Med Phys. 2009; 36: 1602-1609.

19. Sakamoto A, Sakamoto I, Nagayama H, Koike H, Sueyoshi E, Uetani M. Quantification of lung perfusion blood volume with dual-energy CT: assessment of the severity of acute pulmonary thromboembolism. AJR Am J Roentgenol. 2014; 203: 287-291.

20. Toepker M, Moritz T, Krauss B, Weber M, Euller G, Mang T, et al. Virtual non-contrast in second-generation, dual-energy computed tomography: reliability of attenuation values. Eur J Radiol. 2012; 81: e398- e405.

21. Yu L, Leng S, McCollough CH. Dual-energy CT-based monochromatic imaging. AJR Am J Roentgenol. 2012; 199: S9 - S15.

22. Bolus DN. Dual-energy computed tomographic scanners: principles, comparisons, and contrasts. J Comput Assist Tomogr. 2013; 37: 944-947.

23. Mangold S, Gatidis S, Luz O, König B, Schabel C, Bongers MN, et al. Single-source dual-energy computed tomography: use of monoenergetic extrapolation for a reduction of metal artifacts. Invest Radiol. 2014; 49: 788-793.

24. Ginat DT, Gupta R. Advances in computed tomography imaging technology. Annu Rev Biomed Eng. 2014; 16: 431-453.

25. Gabbai M, Leichter I, Mahgerefteh S, Sosna J. Spectral material characterization with dual-energy CT: comparison of commercial and investigative technologies in phantoms. Acta Radiol. 2015; 56: 960-969.

26. Higashi Y, Nakamura H, Matsumoto T, Nakanishi T. Dual-energy computed tomographic diagnosis of pulmonary nodules. J Thorac Imaging. 1994; 9: 31-34.

27. Bhalla M, Shepard JA, Nakamura K, Kazerooni EA. Dual kV CT to detect calcification in solitary pulmonary nodule. J Comput Assist Tomogr. 1995; 19: 44-47.

28. Swensen SJ, Yamashita K, McCollough CH. Lung nodules: dual-kilovolt peak analysis with CT--multicenter study. Radiology. 2000; 214: 81-85.

29. Chae EJ, Song JW, Seo JB, Krauss B, Jang YM, Song KS. Clinical utility of dual-energy CT in the evaluation of solitary pulmonary nodules: initial experience. Radiology. 2008; 249: 671-681.

30. Knoss N, Hoffmann B, Krauss B, Heller M, Biederer J. Dual energy computed tomography of lung nodules: differentiation of iodine and calcium in artificial pulmonary nodules in vitro. Eur J Radiol. 2011; 80: e516- e519.

31. Kawai T, Shibamoto Y, Hara M, Arakawa T, Nagai K, Ohashi K. Can dual-energy CT evaluate contrast enhancement of ground-glass attenuation? Phantom and preliminary clinical studies. Acad Radiol. 2011; 18: 682-689.

32. Iwano S, Ito R, Umakoshi H, Ito S, Naganawa S. Evaluation of lung cancer by enhanced dual-energy CT: association between three-dimensional iodine concentration and tumour differentiation. Br J Radiol. 2015; 88: 20150224.

33. Schmid-Bindert G, Henzler T, Chu TQ, Meyer M, Nance JW Jr, Schoepf UJ, et al. Functional imaging of lung cancer using dual energy CT: how does iodine related attenuation correlate with standardized uptake value of 18FDG-PET-CT? Eur Radiol. 2012; 22: 93-103.

34. Hou WS, Wu HW, Yin Y, Cheng JJ, Zhang Q, Xu JR. Differentiation of lung cancers from inflammatory masses with dual-energy spectral CT imaging. Acad Radiol. 2015; 22: 337-344.

35. Yanagita H, Honda N, Nakayama M, Watanabe W, Shimizu Y, Osada H, et al. Prediction of postoperative pulmonary function: preliminary comparison of single-breath dual-energy xenon CT with three conventional methods. Jpn J Radiol. 2013; 31: 377- 385.

36. Chae EJ, Kim N, Seo JB, Park JY, Song JW, Lee HJ, et al. Prediction of postoperative lung function in patients undergoing lung resection: dual-energy perfusion computed tomography versus perfusion scintigraphy. Invest Radiol. 2013; 48: 622-627.

37. Li GJ, Gao J, Wang GL, Zhang CQ, Shi H, Deng K. Correlation between vascular endothelial growth factor and quantitative dual-energy spectral CT in non-small-cell lung cancer. Clin Radiol. 2016; 71: 363-368.

38. Ogawa M, Hara M, Imafuji A, Ozawa Y, Arakawa T, Kobayashi S, et al. Dual-energy CT can evaluate both hilar and mediastinal lymph nodes and lesion vascularity with a single scan at 60 seconds after contrast medium injection. Acad Radiol. 2012; 19: 1003-1010.

39. Imafuji A, Hara M, Sasaki S, Arakawa T, Ozawa Y, Shibamoto Y. Usefulness of dual-energy CT scanning at 80 kVp for identifying hilar and mediastinal structures: evaluation of contrast enhancement of the pulmonary vessels and lymph nodes. Jpn J Radiol. 2012; 30: 69-77.

40. Lee SH, Hur J, Kim YJ, Lee HJ, Hong YJ, Choi BW. Additional value of dual-energy CT to differentiate between benign and malignant mediastinal tumors: an initial experience. Eur J Radiol. 2013; 82: 2043-2049.

41. Chang S, Hur J, Im DJ, Suh YJ, Hong YJ, Lee HJ, et al. Dual-energy CT-based iodine quantification for differentiating pulmonary artery sarcoma from pulmonary thromboembolism: a pilot study. Eur Radiol. 2015.

42. Baxa J, Vondráková A, Matoušková T, Růžičková O, Schmidt B, Flohr T , et al. Dual-phase dual-energy CT in patients with lung cancer: assessment of the additional value of iodine quantification in lymph node therapy response. Eur Radiol. 2014; 24: 1981-1988.

43. Baxa J, Matouskova T, Krakorova G, Schmidt B, Flohr T, Sedlmair M, et al. Dual-Phase Dual-Energy CT in Patients Treated with Erlotinib for Advanced Non-Small Cell Lung Cancer: Possible Benefits of Iodine Quantification in Response Assessment. Eur Radiol. 2015.

44. Kim YN, Lee HY, Lee KS, Seo JB, Chung MJ, Ahn MJ, et al. Dual-energy CT in patients treated with anti-angiogenic agents for non-small cell lung cancer: new method of monitoring tumor response? Korean J Radiol. 2012; 13: 702-710.

45. Gutjahr R, Halaweish AF, Yu Z, Leng S, Yu L, Li Z, et al. Human Imaging With Photon Counting-Based Computed Tomography at Clinical Dose

Levels: Contrast-to-Noise Ratio and Cadaver Studies. Invest Radiol. 2016; 51: 421-429.

46. Yu Z, Leng S, Jorgensen SM, Li Z, Gutjahr R, Chen B, et al. Evaluation of conventional imaging performance in a research whole-body CT system with a photon-counting detector array. Phys Med Biol. 2016; 61: 1572-1595.

47. McCollough CH, Leng S, Yu L, Fletcher JG. Dual- and Multi-Energy CT: Principles, Technical Approaches, and Clinical Applications. Radiology. 2015; 276: 637-653.

48. Pourmorteza A, Symons R, Sandfort V, Mallek M, Fuld MK, Henderson G, et al. Abdominal Imaging with Contrast-enhanced Photon-counting CT: First Human Experience. Radiology. 2016; 279: 239-245.

49. Zhu J, Penfold SN. Dosimetric comparison of stopping power calibration with dual-energy CT and single-energy CT in proton therapy treatment planning. Med Phys. 2016; 43: 2845.

50. van Elmpt W, Landry G, Das M, Verhaegen F. Dual energy CT in radiotherapy: Current applications and future outlook. Radiother Oncol. 2016; 119: 137-144.